

Dynamic Modulation of the Regulatory Domain of Myosin Heads by pH, Ionic Strength, and RLC Phosphorylation in Synthetic Myosin Filaments[†]

Bishow B. Adhikari,[‡] Joshua Somerset,[‡] James T. Stull,[§] and Piotr G. Fajer^{*‡}

The National High Magnetic Field Laboratory, Institute of Molecular Biophysics, and Department of Biological Science, Florida State University, Tallahassee, Florida 32306, and Department of Physiology, University of Texas Southwestern Medical Center at Dallas, Dallas, Texas 75235

Received October 27, 1998; Revised Manuscript Received December 17, 1998

ABSTRACT: The position of the myosin head with respect to the filament backbone is thought to be a function of pH, ionic strength (μ) and the extent of regulatory light chain (RLC) phosphorylation [Harrington (1979) *Proc. Natl. Acad. Sci. U.S.A.* 76, 5066–5070]. The object of this study is to examine the dynamics of the proximal part of the myosin head (regulatory domain) which accompany the changes in head disposition. The essential light chain was labeled at Cys177 with the indanedione spin-label followed by the exchange of the labeled proteins into myosin. The mobility of the labeled domain was investigated with saturation transfer electron paramagnetic resonance in reconstituted, synthetic myosin filaments. We have found that the release of the heads from the myosin filament surface by reduction of electrostatic charge is accompanied by a 2-fold increase in the mobility of the regulatory domain. Phosphorylation of the RLC by myosin light chain kinase resulted in a smaller 1.5-fold increase of motion, establishing that the head disordering observed by electron microscopy [Levine et al. (1996) *Biophys. J.* 71, 898–907] is due to increased mobility of the heads. This result indirectly supports the hypothesis that the RLC phosphorylation effect on potentiation of force arises from a release of heads from the filament surface and a shift of the heads toward actin.

The charge balance between the myosin filament surface, the myosin head, and the S2¹ region of myosin defines head disposition with respect to the filament. The [H⁺], ionic strength, divalent ions, and phosphorylation of regulatory light chain (RLC) all change the electrostatics of interacting surfaces. The change of two charges in the S2 region was postulated by Harrington and co-workers to evoke a transition between a “locked” configuration where myosin heads are lying on the surface and a “released”, open configuration, with myosin heads displaced from the filament surface (reviewed in 8). The locked configuration was characterized by low rates of proteolysis of the LMM/HMM junction, a high level of S2 cross-linking to the myosin backbone, and well-ordered myosin heads on the surface of the filaments

as seen by electron microscopy. The release of the heads from the surface induced by lowering [H⁺] and [Mg²⁺], increasing ionic strength, or phosphorylation resulted in loss of protection to proteolysis, reduced cross-linking, and displacement of heads away from the surface (2, 3, 6, 9–13).

The physiological significance of these changes is unclear although increased mobility of the head might facilitate actomyosin interactions at the distal end. In smooth muscle, phosphorylation relieves the inhibition of actomyosin ATPase and initiates contraction. In skeletal muscle, the effects are less dramatic—phosphorylation increases the Ca²⁺ sensitivity and the rate of force regeneration after shortening (14–16). RLC spans the hinge between the S1 and S2 regions of myosin and thus is strategically placed to control the flexibility of this junction (17, 18). Hinge flexibility in turn might modulate interactions of adjacent myosin heads which are implicated in the smooth muscle activation (19–22). Phosphorylation neutralizes the positive charge of amino acids in the vicinity of the phosphorylatable serine and thus disrupts interactions between the head and the filament surface or between the two heads (23). In either case, the motional freedom of the head should increase substantially. Strong support for this hypothesis comes from EM studies of native thick filaments showing an increase in disorder of the myosin head following phosphorylation (6, 24, 25). The head disorder and displacement from the surface of the filament have been interpreted as an increased mobility, motivating this study to measure motion directly by saturation transfer EPR.

[†] Research sponsored by National Science Foundation Grant NSF-IBN-9507477, an NHMFL in-house grant, American Heart Association Grant GIA-9501335, and Grant NIH HL26043. An American Cancer Society Fisher Undergraduate Fellowship awarded to J.S. is also acknowledged.

^{*} To whom correspondence should be addressed. E-mail: fajer@magnet.fsu.edu.

[‡] Florida State University.

[§] University of Texas Southwestern Medical Center at Dallas.

¹ Abbreviations: ATP, adenosine 5'-triphosphate; ADP, adenosine 5'-diphosphate; DTT, dithiothreitol; DITC, diisothiocyanate; EDTA, ethylenediaminetetraacetic acid; EGTA, ethylene glycolbis(β -aminoethyl ether)-N,N',N''-tetraacetic acid; MOPS, 3-(N-morpholino)propanesulfonic acid; InVSL, 2-[oxyl-2,2,5,5-tetramethyl-3-pyrrolin-3-methynyl]indane-1,3-dione; EPR, electron paramagnetic resonance; ST-EPR, saturation transfer electron paramagnetic resonance; RLC, regulatory light chain; ELC, essential light chain; S1, myosin subfragment 1; S2, myosin subfragment 2; LMM, light meromyosin; HMM, heavy meromyosin.

In addition, we have measured the mobility of the heads released from the surface by increases in ionic strength and pH. This study follows that of Ludescher et al. (5), who measured the mobility of the catalytic domain by transient absorption anisotropy. The observed mobility followed the expectation of increased rotational freedom of the "released" heads. The surprising result was the observation of significant microsecond mobility in the "locked" state (5). Since we have recently postulated the presence of a flexible hinge between the regulatory and catalytic domains (26) with the catalytic domain moving 3 times faster than the regulatory domain, this faster motion of the catalytic domain might have obscured the effects of S2/S1 interactions with the filament surface. Thus, we extended Ludescher's investigation to the regulatory domain as that domain being proximal to the filament backbone might display larger motional constraints and be more sensitive to the head-myosin filament backbone interactions.

METHODS

Protein Purification. All preparations and experiments were carried out at 4–6 °C. Myosin was obtained from the back muscles of adult white New Zealand rabbits using standard methods of extraction (Guba–Straub solution: 0.3 M KCl, 0.05 M K_2HPO_4 , 0.1 M KH_2PO_4) and purification by repeated polymerization–depolymerization cycles in low and high ionic strength buffers (27). Essential light chain mixture (ELC) was isolated from purified myosin using the procedure described by Wagner (28) with minor modifications. To remove most of the RLC from the heavy chain, myosin (10–15 mg/mL in 0.5 M KCl, 20 mM Tris-HCl buffer, pH 8.6) was treated with 10 mM EDTA and 10 mM DTNB for 10 min. The free light chains and myosin were separated by 14-fold dilution in 2 mM EDTA, and collected by centrifugation at 10000g for 20 min. This process was repeated to increase the efficiency of RLC removal (up to 90–95% as examined by 12% SDS–PAGE). The resulting pellet was dissolved (in 0.6 M KCl, 20 mM Tris-HCl, pH 8.6), treated with 5 mM DTT for 20 min, and taken through another cycle of filament formation and centrifugation. To isolate ELC, the sample (now mostly RLC-free myosin heavy chain) was treated with 4.5 M guanidine hydrochloride in 0.3 M KCl, 5 mM EDTA, 5 mM DTT, 45 mM Tris-HCl, pH 8.6, overnight, followed by removal of the heavy chain by 66% ethanol precipitation (30 min) and centrifugation (10000g for 20 min). Ethanol and guanidine hydrochloride were removed by rotary evaporation and extensive dialysis in 5 mM phosphate buffer, 1 mM NaN_3 , and 0.1 mM DTT at pH 7.0. Residual heavy chain, which precipitated during the dialysis, was removed by centrifugation. ELC was concentrated to 1–2 mg/mL by vacuum centrifugation and dialyzed against 5 mM sodium phosphate buffer and 0.1 mM DTT (storage buffer) prior to storage at –70 °C.

Essential light chains were separated into LC1 and LC3 by Mono-Q (HR 5/5, Pharmacia) anion-exchange chromatography. The light chain mixture, 1–2 mg/mL, was dialyzed against 0.1 mM DTT and 50 mM sodium phosphate buffer, pH 6.0, and loaded onto the column preequilibrated in the same buffer. The light chains, monitored at 230 nm, were eluted with a 40 min linear gradient of 50–400 mM sodium phosphate buffer, pH 6.0. The addition of 2–5 mM DTT to the protein sample prior to loading in the column was found

to greatly facilitate the separation. The separation resulted in five distinct protein peaks, which upon analysis by SDS–PAGE indicated pure LC1 in the first and largest peak, moderately pure LC2 in the smaller second peak, and mixtures of LC1, -2, and -3 in the three last smaller peaks. Pure LC1 (collected from fractions within the first peak) was dialyzed in the storage buffer, concentrated by vacuum centrifugation to 1–2 mg/mL, dialyzed again in the storage buffer, and stored at –70 °C.

Spin-Labeling and Formation of Synthetic Filaments. Purified LC1 was labeled with a 5-fold molar excess of InVSL (gift of Prof. K. Hidag, University of Pecs) in 40 mM KCl, 0.2 mM EDTA, 1 mM NaN_3 , and 5 mM sodium phosphate buffer, pH 7.0, for 5 h. Excess label was removed by dialysis. The extent of labeling, typically 80–100%, was measured by EPR to quantify the total spin-label concentration and by BCA protein assay (Pierce) to quantify protein concentration.

InVSL-labeled LC1 was exchanged with unlabeled ELC in myosin using the dissociant NH_4Cl as follows (28): InVSL-LC1 (1–2 mg/mL) was dialyzed in 2 mM EDTA, 2 mM DTT, 100 mM MOPS, pH 7.0, and solid NH_4Cl (4.7 M) was added and gently shaken. Myosin in 0.6 M KCl, 20 mM MOPS, pH 7.0, was added at a 5:7 LC1:myosin ratio and allowed to exchange for 30 min while gently shaking, followed by dialysis in 50 mM MOPS, 0.1 mM DTT, pH 7.0, to form synthetic filaments. Excess InVSL-LC1 and displaced endogenous ELC were removed by centrifugation (10000g, 10 min). All EPR experiments were carried out in filaments that were gently pelleted (5000–6000g for 10 min) in a table-centrifuge and loaded into 50 μ L fused silica capillary tubes (Wilma Glass Co., Buena, NJ).

Phosphorylation and Dephosphorylation. RLC of myosin (in 40 mM KCl, 10 mM MOPS, pH 7.0) was phosphorylated in the synthetic filaments following the reconstitution with labeled LC1. Phosphorylation was accomplished by the addition of 1 nM MLCK, 100 nM CaM, 5 mM MgATP, and 1 mM $CaCl_2$ for 20 min at 25 °C or for 12 h at 4 °C. Myosin was dephosphorylated by incubation with alkaline phosphatase (Sigma) in 0.6 M KCl, 20 mM Tris-HCl, pH 8.6, 12.5 mM $CaCl_2$, and 1 mM EGTA (60 units/mL/30 mg of myosin) for 20 min at 30 °C.

2D Gel Electrophoresis. The extent of phosphorylation was examined by 2D gel electrophoresis (Mini-PROTEAN II 2-D system, Bio-Rad Inc.). The first-dimension IEF tube gels (monomer solution composition: 9.2 M urea, 4% acrylamide, 20% Triton X-100, 1.6% Bio-Lyte 5/7 ampholyte, 0.4% Bio-Lyte 3/10 ampholyte, 0.01% ammonium persulfate, 0.1% TEMED) were cast prior to use and kept at 4 °C for up to 2 weeks. Before running the sample, the tube gels were pre-electrophoresed (upper and lower chamber buffer, 100 mM NaOH and 10 mM H_3PO_4 , respectively) at 200 V for 10 min, 300 V for 15 min, and 400 V for 15 min. Approximately, 20–30 μ g of myosin (in 0.6 M KCl, 20 mM MOPS, pH 7.0, myosin buffer) plus an equal volume of first-dimension sample buffer (9.5 M urea, 2% Triton X-100, 5% DTT, 1.6% Bio-Lyte 5/7 ampholyte, 0.4% Bio-Lyte 3/10 ampholyte) with a total sample volume of ~25 μ L was loaded into each of the first-dimension capillary gels and overlaid with 20–40 μ L of sample overlay buffer (9 M urea, 0.8% Bio-Lyte 5/7 ampholyte, 0.2% Bio-Lyte 3/10 ampholyte, and 0.002% bromophenol blue). Isoelectric focusing

was carried out at 750 V for 3–5 h. Following IEF, the gels were removed from the capillary tubes and loaded into SDS–PAGE slab gels (7.5% stacking and 12% main gels), with the molecular weight controls LC1 and LC3 running in the side well. The second-dimension SDS–PAGE was performed under standard conditions (29).

The extent of RLC phosphorylation was measured densitometrically by scanning gels on a page scanner (Microtek III) at 600 dpi resolution using the Adobe Photoshop software (Adobe Systems, Inc.). The images were saved as TIFF files. Global Lab Image software, version 2.1 (Data Translation, Inc.), was used to generate the density profiles across the long and short axes for each protein spot (elliptic shape) in the image. The volumes enclosed within the profiles were then computed using MathCAD software (MathSoft Inc., 5.0) so as to determine the relative percentage of phosphorylated and unphosphorylated RLC within the same gel.

EPR and ST-EPR Spectroscopy. All EPR and ST-EPR experiments were performed on a Bruker ECS-106 spectrometer (Bruker Instruments, Billerica, MA) as in Adhikari and Fajer (30), using a TE₁₀₂ cavity with a microwave field strength (H_1) of 0.03–0.08 G and a static field modulation amplitude (H_m) of 2 G for EPR and $H_1 = 0.25$ G and $H_m = 5$ G for ST-EPR. The modulation frequency was 50 kHz. All experiments were carried out at 4 °C in 50 mM MOPS, 0.1 mM DTT, pH 7.0, unless otherwise specified. ST-EPR spectra were analyzed by comparison to spectra of InVSL-labeled hemoglobin tumbling in a media of known viscosity (87.55 wt %/wt, glycerol/water mixture, –30 °C to 20 °C) (31).

RESULTS

Myosin light chain 1 (LC1) was labeled specifically with indanedione spin-label (InVSL) at the unique Cys177 and exchanged into myosin. As we have shown previously (26), this particular label reports on the microsecond mobility of the regulatory domain with no indication of faster nanosecond motions of the label with respect to protein.² Therefore, in the remainder of the paper we will refer to regulatory domain mobility as being measured by the mobility of InVSL-LC1.

Ionic Strength and pH Effects. The effect of increasing ionic strength (μ) on the dynamics of the regulatory domain is shown in Figure 1. There is a significant difference in the ST-EPR line shape between the spectra at $\mu = 45$ mM and 200 mM; high μ spectra have lower intensity at the diagnostic regions L'', C', and H''. Diagnostic regions correspond to the areas of high spectral diffusion and are most sensitive to rotational motion (33). To remove the dependence on effects other than motion, it is customary to normalize the intensity of the diagnostic regions to that of “turning points” (L, C, and H in Figure 1) for which spectral diffusion is minimal. Thus, the normalized line height ratios are primarily sensitive to rotational diffusion. In this work, we chose to report the values from the low-field region (L''/L) as they are less influenced by spectral overlap than the central field (31, 34)

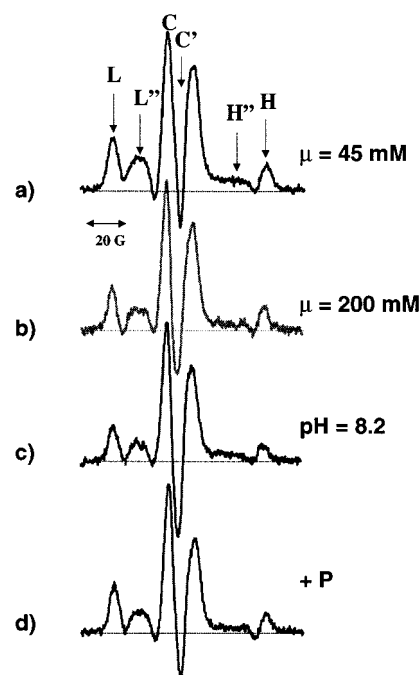


FIGURE 1: (A) ST-EPR spectra of InVSL-ELC-labeled myosin filaments: (a) ionic strength (μ) was 45 mM; (b) $\mu = 200$ mM; (c) pH = 8.2; (d) phosphorylated. The lower intensity at L'' (normalized to intensity at L) indicates higher mobility.

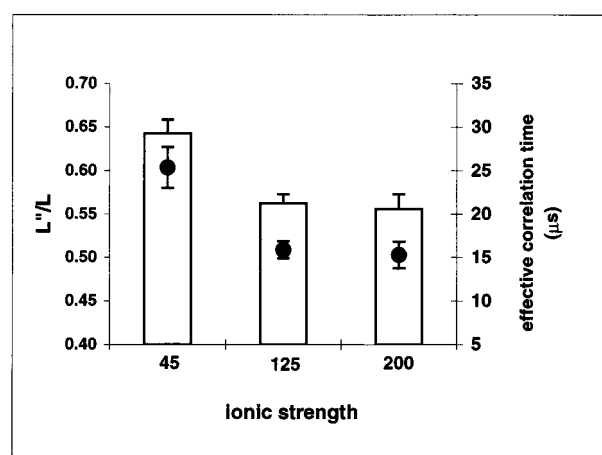


FIGURE 2: Comparison of mobility of InVSL-ELC-labeled myosin filaments at three differing ionic strength conditions. The open bars and ordinate on the left represent the low-field peak height ratios (L''/L); the circles and ordinate on the right represent the corresponding effective rotational correlation times (τ_R) in microseconds. The error bars represent \pm SEM of 3–5 independent measurements. Note that lower τ_R correspond to faster motions.

and have 3 times higher signal-to-noise ratio than the high field region (H''/H).

For synthetic filaments, the ratios L''/L at $\mu = 45$ and 200 mM are 0.64 and 0.56 (Figure 2). These differences are statistically significant ($p = 0.002$), and they indicate that the mobility at $\mu = 200$ mM is higher than at $\mu = 45$ mM. The effective correlation times (τ_R), obtained by comparison of the L''/L ratio in myosin with that of InVSL hemoglobin tumbling in a glycerol/water mixture of known viscosity, are $\tau_R = 25.3 \pm 4 \mu$ s at $\mu = 45$ mM and $15.3 \pm 2 \mu$ s at 200 mM. The increase of mobility is consistent with the weakening of the electrostatic attraction between the head and filament surface as found by Harrington (1).

² We note that smaller labels (iodoacetamide, iodo keto- or maleimido-derivatives) were not as sterically constrained and they all exhibited nanosecond motion characteristic of either independent motion of the label or the motion of cysteine (32).

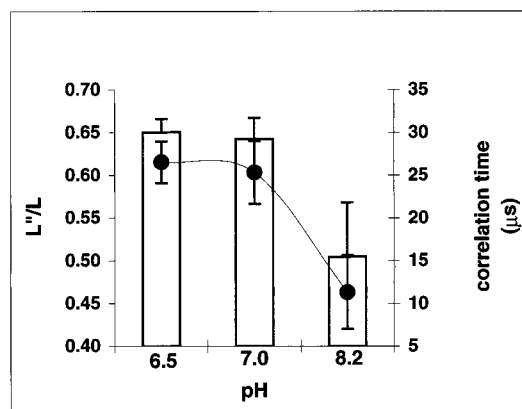


FIGURE 3: Mobility of InVSL-ELC-labeled myosin filaments at three pH values. The bars and ordinate on the left are the L''/L ratios, while the ordinate on the right and the circles represent the corresponding effective rotational correlation times in microseconds.

Table 1: Effective τ_R of InVSL-ELC-Labeled Myosin Filaments

sample	μ (mM)	pH	L''/L	error (SEM)	τ_R (μs)	error (SEM)	n	Student's t -test, ^a p =
unphosphorylated	45	7	0.64	0.02	25.3	3.7	5	N/A
	125	7	0.56	0.01	15.9	1.0	3	0.001
	200	7	0.56	0.02	15.3	1.5	3	0.002
	45	6.5	0.65	0.02	26.5	2.5	4	N/A
	45	8.2	0.50	0.06	11.3	4.3	3	0.002
dephosphorylated	45	7	0.65	0.01	26.2	2.0	4	N/A
phosphorylated	45	7	0.57	0.02	16.9	1.8	4	0.002

^a t -test taken in nonaveraged spectra.

The charge balance is also affected by increasing $[H^+]$ (9). ST-EPR spectra at pH 6.5 and 8.2 ($\mu = 45$ mM) are shown in Figure 1a,b. The spectrum at pH 8.2 was significantly different from that at lower pH, with decreased L'' intensity. This change corresponds to a 2-fold increase of mobility at pH 8.2 as compared to the mobility at pH 6.8 (or pH 7.0) (Figure 3), Table 1.

Thus, the effects of increasing pH and of increasing ionic strength are the same as originally reported for the catalytic domain (5). The regulatory domain where our signals originate seems to be affected by the unlocking of the heads in the same fashion as the catalytic domain.

Phosphorylation of RLC. Phosphorylation of the regulatory domain has been shown to result in the movement of myosin heads away from the filament surface (6). Looking for the associated changes in protein dynamics, we have compared the mobility of phosphorylated and dephosphorylated myosin.

Ser16 of RLC was phosphorylated in myosin with myosin light chain kinase to 75–85% as determined from densitometric analysis of the 2D gels which resolve the phosphorylated and unphosphorylated forms of RLC (Figure 4). Since our purified myosin was typically ~20% phosphorylated, we have used alkaline phosphatase to fully dephosphorylate the protein.

Figure 1d shows a ST-EPR spectrum of phosphorylated myosin filaments, $\mu = 45$ mM and pH 7.0. As for increasing μ or pH, L'' intensity is lower than for the unphosphorylated filaments in Figure 1a. The correlation time for the phosphorylated myosin, $\tau_R = 16.9 \pm 2 \mu s$ is smaller (motion is faster) than $26.2 \pm 2 \mu s$ for the dephosphorylated myosin (Table 1). These results suggest that the EM observed disordering of the heads (6) is associated with increased head mobility.

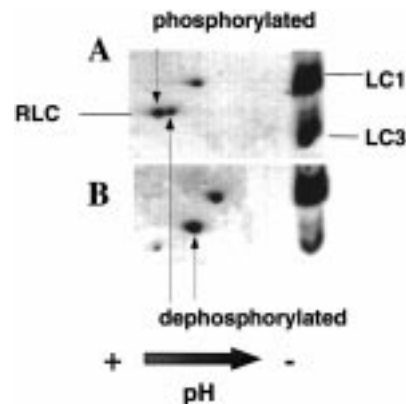


FIGURE 4: IEF-SDS-PAGE of phosphorylated (A) and dephosphorylated (B) myosin. 75–85% of RLC was phosphorylated as estimated by densitometry.

DISCUSSION

The myosin structure and function are modulated by variations in ionic strength, pH, the presence of divalent cations, and the extent of RLC phosphorylation. In skeletal muscle these variables change the positions of S1 and S2 domains relative to the filament backbone and they increase Ca^{2+} sensitivity and rate of force development. The present study demonstrates that the structural and functional modulation of the myosin head relative to the filament backbone is correlated to its degree of motional freedom at the regulatory domain. In particular, we have shown directly using a motionally sensitive technique, ST-EPR, that the conditions which are known to release myosin heads from the filament surface increase the mobility of the regulatory domain.

Effects of Ionic Strength and pH. Weak attraction between the carboxy-terminal segment of S2, near the S2/LMM proteolytic site, and the myosin filament backbone is thought to occur via electrostatic charges on the surfaces of these myosin domains (reviewed in 8). Cross-linking and proteolysis rates in synthetic myosin, synthetic rods, and myofibrils all demonstrate that this interaction is modulated by the medium's ionic strength and pH (2, 3, 9, 11, 35). On the basis of these experiments, it has been postulated that at low ionic strength or neutral pH, S2 is bound to the filament backbone and an increase of ionic strength or deprotonation weakens these electrostatic interactions ($2H^+$ change in charge balance) and “unlocks” S2 from the thick filament surface (9). The precise source of these electrostatic interactions is not known, but there are a number of positively and negatively charged areas both on the filament surface and on the regulatory domain. One can speculate that the deprotonation of specific, positively charged residues near-neutral pH might abolish such an interaction and release S2 from the filament surface. At the time, the correlation between the activation energy for head release and for the melting of the α -helical stretch in S2 implicated the process in force generation (1, 36). Even if force is not produced in that event, it is hard to believe that such a profound structural change would not modulate muscle function. Indeed, similar events accompanying phosphorylation increase the rate of force development (15, 16).

The study of Ludescher et al. (5) showed that displacement of the heads from the filament surface was accompanied by an increase of the mobility of the catalytic domain. The

decrease of pH, ionic strength, and binding of divalent ions resulted in 2-fold slower motions. However, as the authors pointed out, the observed microsecond motion in the "locked" state was still significantly (~ 10 – 20 -fold) faster than the fastest motions predicted for the filament itself (37, 38). The fast rate of motion and the large amplitude imply large motional freedom of the heads when bound to the filament surface. A possibility advanced by Ludescher et al. (5) was that the catalytic domain where the label was placed was moving independently from the S2 region which interacted with the filament surface. Recently we have found a flexible hinge between the catalytic and regulatory domains (26) which prompted us to investigate the mobility of the regulatory domain. The regulatory domain rather than the distal catalytic domain should be more sensitive to the interactions with the thick filament surface. However, the mobility of the regulatory domain of the heads in the "locked" state, although slower than that of the catalytic domain, is still much faster ($25.3 \mu\text{s}$) than the filament mobility which we measured previously ($\tau_r = 150 \mu\text{s}$, 26), very much in agreement with the original findings of Ludescher et al. (5) of the catalytic domain. Moreover, the 2-fold mobility changes observed on the catalytic domain are the same as the changes observed here on the regulatory domain. This result suggests that (a) the myosin head experiences large motional freedom even when interacting with the filament surface and (b) interactions of the catalytic and regulatory domains with the surface are similar; i.e., the catalytic–regulatory domain hinge is not affected by ionic strength or proton concentration. The significance of these findings lies in excluding the possibility that the stiffness of the myosin head is modulated by filament surface–myosin head interactions. Modulation of stiffness of any linkage between the motor domain and the filament to which the force is transmitted would have had a profound impact on any of the current molecular models of force generation in muscle.

RLC Phosphorylation. Phosphorylation of smooth muscle results in the dramatic structural transition between the folded 10S and extended 6S conformations (39–41). In skeletal muscle, the changes are not as dramatic, but still phosphorylation of Ser16 of RLC decreased the efficiency of cross-linking of S2 and the filament surface and promoted proteolysis at the LMM/HMM junction (2, 4).

As these effects are analogous to those induced by pH and ionic strength, it was postulated that the head is also released from the filament surface (4). This notion was recently confirmed by electron microscopy. Levine and co-workers (6, 24, 25) have observed disordering of the myosin heads in electron micrographs of native thick filaments from skeletal muscle which accompanied phosphorylation of the LC2 by myosin light chain kinase. Assuming that the phosphorylation-induced structural changes are similar in native and synthetic myosin filaments, our results show that the observed disorder is dynamic. When S2 is displaced away from the filament surface, the heads gain a larger degree of rotational freedom (EM) as reflected by increased mobility (ST-EPR). Although larger mobility was postulated before (4, 6), the current finding is the first direct measurement of such an increase in mobility.

One can only speculate on the functional significance of that mobility. Sweeney et al. (7) postulated that movement

of the heads toward actin promotes actomyosin interactions. The proximity to actin accounts for posttetanic potentiation of twitch tension (42), tension potentiation at submaximal activation (14) due to the increased affinity and rate of force development (15, 16). Strong support for the "actin proximity" argument was recently established by Yang et al. (43), who mimicked the phosphorylation effects with the decreased lattice spacing. We note that our results only indirectly support these functional implications of crossbridge mobility. Mobility changes observed in synthetic filaments do not necessarily translate into similar changes within fiber lattice constraints. To make the correlation with observed physiological effects, one would need to perform a similar study in muscle fibers; such a study is currently in progress.

The molecular origin of phosphorylation effects is unclear. Studies of Sweeney et al. (23) implied that the phosphorylation reduces a net positive charge at the N-terminus of RLC, lessening attraction with putative negative charges in the filament backbone. Scallop muscle fibers with RLC mutants carrying less charge in the N-terminal region displayed force potentiation similar to that of phosphorylated myosin. However, ATPase activities and in vitro motility in smooth muscle were not activated by the charge reduction—these processes required actual phosphorylation (23). Similar, complex behavior was noted on comparison of tension profiles of muscles reconstituted with skeletal and smooth RLC (25). Smooth muscle RLC contains more basic residues than skeletal RLC, yet its profile is more like that induced by phosphorylation. It is quite likely that the phosphorylation decreases the positive charge of RLC and thereby reduces interaction with the filament surface or with the other myosin head (44). Weakened protein–protein interactions in turn result in the increased head mobility observed here.

In summary, the present study demonstrates that the regulatory domain dynamics is related to the conformation of the myosin filament. When the electrostatic interactions of S2 with the filament surface are weakened by increasing ionic strength or $[\text{H}^+]$ and the myosin heads are "unlocked" from the surface, their mobility increases 2-fold. A similar effect is observed on phosphorylation of RLC. These observations indirectly support the hypothesis that the increased mobility and displacement of myosin heads from the myosin filaments promote actomyosin interactions and thus might modulate force generation (7).

ACKNOWLEDGMENT

We thank Dr. Brett Hambly for many discussions and Elizabeth Fajer, Dr. Hui Li, and April Adhikari for technical help and editorial assistance.

REFERENCES

- Harrington, W. F. (1979) *Proc. Natl. Acad. Sci. U.S.A.* 76, 5066–5070.
- Ritz-Gold, C. J., Cooke, R., Blumenthal, D. K., and Stull J. T. (1980) *Biochem. Biophys. Res. Commun.* 93, 209–214.
- Reisler, E., and Liu, J. (1982) *J. Mol. Biol.* 157, 659–669.
- Mrakovcic-Zenic, M. A., and Reisler, E. (1983) *Biochemistry* 22, 525–530.
- Ludescher, R. D., Eads, T. M., and Thomas, D. D. (1988) *J. Mol. Biol.* 200, 89–99.
- Levine, R. J. C., Kensler, R. W., Yang, Z., Stull, J. T., and Sweeney, H. L. (1996) *Biophys. J.* 71, 898–907.

7. Sweeney, H. L., Bowman, B. F., and Stull, J. T. (1993) *Am. J. Physiol.* 264, C1085–C1095.
8. Harrington, W., Rodgers, M. E., and Davis, J. S. (1990) in *Molecular mechanisms in muscular contraction* (Squire, J. M., Ed.) pp 241–263, The Macmillan Press Ltd., London.
9. Ueno, H., and Harrington, W. F. (1981) *J. Mol. Biol.* 149, 619–640.
10. Ueno, H., and Harrington, W. F. (1984) *J. Mol. Biol.* 180, 667–701.
11. Sutoh, K., Chiao, Y. C., and Harrington, W. F. (1978) *Biochemistry* 17, 1234–1239.
12. Borejdo, J., and Werber, M. M. (1982) *Biochemistry* 21, 549–555.
13. Reisler, E., Liu, J., and Cheung, P. (1983) *Biochemistry* 22, 4954–4960.
14. Sweeney, H. L., and Stull, J. T. (1986) *Am. J. Physiol.* 250, C657–C660.
15. Sweeney, H. L., and Stull, J. T. (1990) *Proc. Natl. Acad. Sci. U.S.A.* 87, 414–418.
16. Metzger, J. M., Greaser, M. L., and Moss, R. L. (1989) *J. Gen. Physiol.* 93, 855–883.
17. Xie, X., Harrison, D. H., Schlichting, I., Sweet, R. M., Kalabokis, V. N., Szent-Gyorgyi, A. G., and Cohen, C. (1994) *Nature* 368, 306–312.
18. Houdusse, A., and Cohen, C. (1996) *Structure* 4, 21–32.
19. Wolff-Long, V. L., Saraswat, L. D., and Lowey, S. (1993) *J. Biol. Chem.* 268, 23162–23167.
20. Trybus, K. M. (1994) *J. Muscle Res. Cell Motil.* 15, 587–594.
21. Ikebe, M., Koretz, J., and Hartshorne, D. J. (1985) *J. Biol. Chem.* 263, 6432–6437.
22. Cremo, C. R., Sellers, J. R., and Facemyer, K. C. (1995) *J. Biol. Chem.* 270, 2171–2175.
23. Sweeney, H. L., Yang, Z., Hz, G., Stull, J. T., and Trybus, K. M. (1994) *Proc. Natl. Acad. Sci. U.S.A.* 91, 1490–1494.
24. Levine, R. J. C., Chantler, P. D., Kensler, R. W., and Woodhead, J. L. (1991) *J. Cell Biol.* 113, 563–572.
25. Levine, R. J. C., Yang, Z., Epstein, N. D., Fananapazir, L., Stull, J. T., and Sweeney, H. L. (1998) *J. Struct. Biol.* 122, 149–161.
26. Adhikari, B., Hideg, K., and Fajer, P. G. (1997) *Proc. Natl. Acad. Sci. U.S.A.* 94, 9643–9647.
27. Margossian, S. S., and Lowey, S. (1982) *Methods Enzymol.* 85 (Part B), 55–71.
28. Wagner, P. D. (1982) *Methods Enzymol.* 85, 72–81.
29. Li, H. C., and Fajer, P. G. (1994) *Biochemistry* 33, 14324–14332.
30. Adhikari, B. B., and Fajer, P. G. (1996) *Biophys. J.* 70, 1872–1880.
31. Fajer, P., and Marsh, D. (1983) *J. Magn. Reson.* 51, 446–459.
32. Mchaourab, H. S., Lietzow, M. A., Hideg, K., and Hubbell, W. L. (1996) *Biochemistry* 35, 7692–7704.
33. Thomas, D. D., Seidel, J. C., Gergely, J., and Hyde, J. S. (1975) *J. Supramol. Struct.* 3, 376–390.
34. Robinson, B. H., and Dalton, L. R. (1980) *J. Chem. Phys.* 72, 1312.
35. Chiao, Y. C., and Harrington, W. F. (1979) *Biochemistry* 18, 959–963.
36. Tsong, T. Y., Karr, T., and Harrington, W. F. (1979) *Proc. Natl. Acad. Sci. U.S.A.* 76, 1109–1113.
37. Emes, C. H., and Rowe, A. J. (1978) *Biochim. Biophys. Acta* 537, 125–144.
38. Suzuki, N., and Wada, A. (1981) *Biochim. Biophys. Acta* 670, 408–420.
39. Trybus, K. M., Huiatt, T. W., and Lowey, S. (1982) *Proc. Natl. Acad. Sci. U.S.A.* 79, 6151–6155.
40. Onishi, H., and Wakabayashi, T. (1982) *J. Biochem. (Tokyo)* 92, 871–879.
41. Craig, R., Smith, R., and Kendrick-Jones, J. (1983) *Nature* 302, 436–439.
42. Manning, D. R., and Stull, J. T. (1982) *Am. J. Physiol.* 242, C234–C241.
43. Yang, Z., Stull, J. T., Levine, R. J. C., and Sweeney, H. L. (1998) *J. Struct. Biol.* 122, 139–148.
44. Saraswat, L. D., and Lowey, S. (1991) *J. Biol. Chem.* 266, 19777–19785.

BI982553G